Temperature-, gate-, and photoinduced conductance of close-packed CdTe nanocrystal films

V. J. Porter,[1,2] T. Mentzel,[1,3] S. Charpentier,[1,3] M. A. Kastner,[1,3] and M. G. Bawendi[1,2]

[1]*Center for Materials Science and Engineering, Massachusetts Institute of Technology, 77 Massachusetts Avenue, Cambridge, Massachusetts 02139, USA*

[2]*Department of Chemistry, Massachusetts Institute of Technology, 77 Massachusetts Avenue, Cambridge, Massachusetts 02139, USA*

[3]*Department of Physics, Massachusetts Institute of Technology, 77 Massachusetts Avenue, Cambridge, Massachusetts 02139, USA*

We measure the conductance of close-packed films of CdTe nanocrystals in field-effect structures in the dark and in the presence of light. We find that the majority carriers are holes, that they are injected from gold electrodes into the CdTe nanocrystal films, and that the hole density can be modulated with gate voltage. Secondary photocurrents have a photoconductive gain of ∼10 at 10^6 V/cm showing that the hole mobility is higher than the electron mobility. A single phenomenological description of the field dependence of the hole mobility can explain the dependence of current on source-drain voltage for both dark and light currents.

I. INTRODUCTION

Colloidal semiconductor nanocrystals (NCs) are fluorescent nanoparticles having a discrete energy structure caused by the confinement of the exciton. The emission from NCs can be tuned by varying their size. Applications for NCs have been demonstrated in a variety of fields ranging from biological imaging[1–8] to novel lasing devices.[9–14] Many of the possible applications for NCs, such as light emitting diodes and photodetectors, involve the transport of charge through films of NCs. Recent research has been directed towards better understanding the electronic conduction in NC films, not only to engineer better devices, but also from a basic scientific interest in how the movement of charge through a solid built of "artificial atoms" differs from conduction in a solid composed of natural atoms.

A roadblock in the study of conductance in NC solids has been the insulating nature of the films. CdSe NC films have been doped with excess charge in an electrochemical cell[15–17] and excess charge created with photoexcitation[18–20] in order to generate currents large enough to study. The magnitude of the photocurrent has been enhanced by annealing the NCs to decrease interdot spacing[21] and, most recently, by a series of postdeposition chemical treatments which increase surface passivation and also decrease interdot spacing. The chemical treatments increase the photocurrent by over three orders of magnitude to levels where it saturates with applied field.[22] The saturation with a photoconductive gain equal to unity shows that the photocurrent in CdSe NC films is primary, meaning charge can be extracted but not injected into the photoconductor from the gold electrodes used in the experiments.[22,23] While high photocurrent with no underlying dark current is an ideal characteristic for an application like photodetection, the fact that gold forms a blocking contact with CdSe NCs limits the study of the intrinsic transport properties of the films.

We find that, unlike the CdSe NC system, CdTe NC films form nonblocking contacts with gold electrodes. In this paper we demonstrate, by making the film the channel of a field effect transistor (FET), that the dominant charge carriers in CdTe NC films are holes and that the density of holes can be changed by applying a voltage to the gate. The effect of trapping on the dark current and photocurrent is discussed, and the results from photocurrent studies on the CdTe NC films are presented. Secondary photocurrents are observed in the CdTe NC films, and they are examined and contrasted with the photocurrent in CdSe NC films. In addition, a single phenomenological description of the field dependence of the rate of tunneling between dots fits the voltage dependence of the current for both the dark current and the photocurrent.

Our paper is organized as follows: In Sec. II we describe the sample preparation and measurement techniques used. Section III provides the results of measurements of dark current as a function of temperature, gate voltage, and source-drain voltage, and photocurrent as a function of source-drain voltage and temperature. Data are provided for samples as prepared and treated with butylamine. In Sec. IV we discuss our results and in Sec. V we summarize our conclusions.

II. EXPERIMENTAL DETAILS

A. Sample preparation

CdTe NCs with a first absorption feature at 680 nm, emission at 698 nm, and average particle diameter of 6.2±0.4 nm are synthesized by substituting a telluride for a sellenide precursor in a previously published procedure for making CdSe NCs.[12] A solution of cadmium 2, 4-pentanedionate (98%), 1, 2-hexadecanediol, and tri-*n*-octylphosphine (TOP) is degassed for 1 h at 100 °C. This solution is cooled under argon and 1.5 M tri-*n*-octylphosphine telluride (TOPTe) added. The mixture is then loaded into syringe and injected into a 360 °C hot solvent solution consisting of 99% tri-*n*-octylphosphine oxide (TOPO), hexadecylamine, and hexaphosphonic acid. The NCs are grown for approximately 10 min at 260 °C and then cooled to room temperature. Hexane is added to the room temperature growth solution and the growth solution is transferred to the nitrogen atmosphere of the glovebox for storage.

5 ml of growth solution is processed via previously reported methods to make close-packed films of NCs.[18–20,22,24–27] The main difference between other proce-
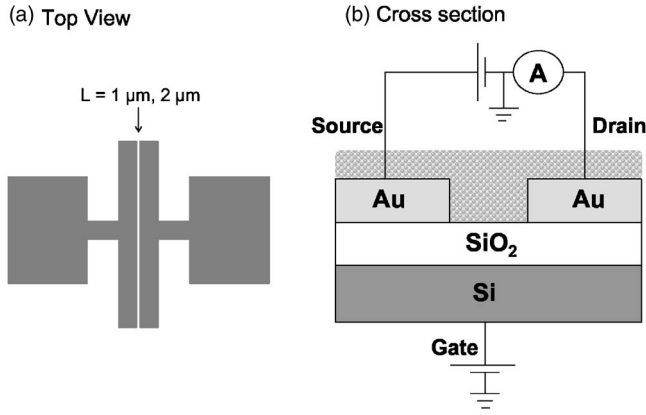
FIG. 1. Top (to scale) (a) and cross-sectional views (not to scale) (b) of the FET measurement device used in the experiments. Gold electrodes $200 \times 800 \times 0.1$ μm^3 are patterned on 330 nm of silicon oxide which is grown on the Si back gate. The electrodes are spaced by 1 or 2 μm. The pads adjacent to the electrodes (a) are used for wire bonding to contact the device to the external circuit. The NC film is drop cast over the entire measurement device and is approximately 150 nm thick when measured from the SiO_2 layer.

dures and the CdTe procedure is that all processing of the CdTe NCs is done air free in the glovebox. The first step is to centrifuge the sample and save the supernatant. The precipitate consisting of TOPO and other salts is discarded. The NCs are next precipitated by adding methanol and spinning the solution in the centrifuge. The supernatant is discarded and the CdTe NCs are dissolved in hexane and butanol. The solution is then filtered through a 0.2 μm filter. The precipitation process is repeated again using 0.1 μm filter. The CdTe NCs are precipitated a third time but they are dissolved in a 9:1 hexane:octane mixture, rather than hexane and butanol, and passed through a 0.02 μm filter. This solution is drop cast onto the measurement device, a silicon inverted field effect transistor (FET).

The FETs are fabricated by lithographically patterning gold bar electrodes $200 \times 800 \times 0.1$ μm^3 on 330 nm of silicon oxide.[28] The electrodes are spaced by 1 or 2 μm. Top and cross sectional views of the electrodes are shown in Fig. 1. The FETs are attached onto a 28-pin chip carrier with silver paint and electrical contacts are made from the electrodes to the chip carrier by gold wire bonds. Devices are tested by applying high voltage to the source, drain, and gate electrodes prior to nanocrystal deposition to screen for leakage pathways between the electrodes and through the oxide. Devices with leakage greater than 0.5 pA are discarded.

The chemical treatment with butylamine involves soaking the CdTe NC film in a 0.1 M solution of butylamine in acetonitrile for 10 min. The film is rinsed with acetonitrile and then dried in the oven for 1 h at 70 °C.

B. Measurements

All conductivity measurements are performed in a Janis VPF-100 cryostat under vacuum. Samples are loaded into the cryostat in the glovebox and are never exposed to air. Current, I, is measured and the drain-source voltage, V_{ds}, is
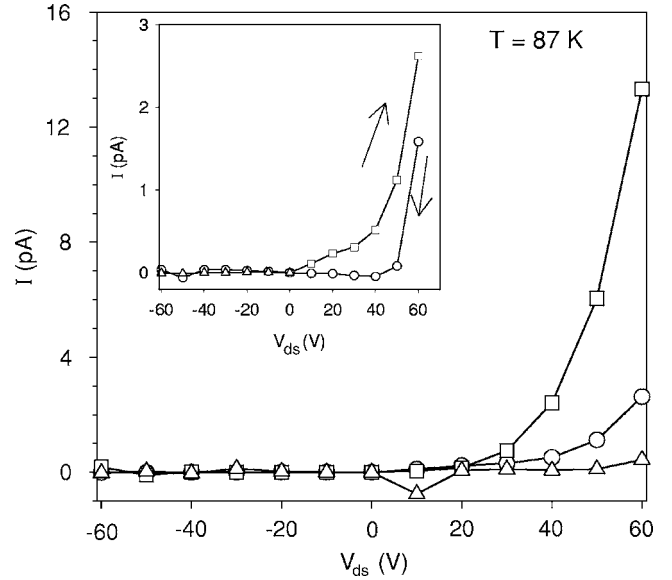

FIG. 2. Dark current, I, at 87 K as a function of drain bias with $V_g = 0$ V (open circles), $V_g = -40$ V (open squares), and $V_g = +40$ V (open triangles). The inset is the full I-V curve with $V_g = 0$ V and it displays the hysteresis present at low temperature. The current is swept from 0 V to +60 V (open squares), from +60 V to −60 V (open circles), and finally from −60 V to 0 V (open triangles) and it is higher on the sweep from 0 to +60 V than when the sweep is reversed. The solid lines serve as guides to the eye.

sourced with a Keithley 6517 electrometer. Gate voltage, V_g, is supplied with an Agilent 6614C DC power supply. A schematic of the electronic setup is given in Fig. 1. An Ar^+ laser at 514 nm is used to photoexcite the samples. It has been shown previously that photocurrent is not a result of photoinjection from the electrodes.[19] The temperature is monitored with a Lakeshore 330 temperature controller. Photocurrent decay measurements are performed by modulating the excitation light with an acousto-optic modulator and monitoring the current with a Keithley 428 current amplifier and Tektronix TDS 7154 oscilloscope.

The differential conductance measurements are carried out by applying a constant V_{ds} with the Agilent 6614C dc power supply. A small ac voltage is added to the drain electrode by a function generator. The resulting ac current is sent to a current amplifier (Ithaco 1211), then to a lock-in amplifier (Princeton Applied Research 5301A), and finally read from a digital multimeter (Hewlett Packard 34401A). V_g is stepped with a Keithley 2400 sourcemeter.

III. RESULTS

Figure 2 shows the dark current through a CdTe NC film versus V_{ds} at 87 K with gate voltage, $V_g = 0$ V (open circles), +40 V (open triangles), and −40 V (open squares). The inset displays the complete I-V curve for the sample with the gate grounded. For the latter, V_{ds} is swept from 0 V to +60 V (open squares), from +60 V to −60 V (open circles), and finally from −60 V back to 0 V (open triangles). The current is hysteretic with more current on the sweep from 0 V to
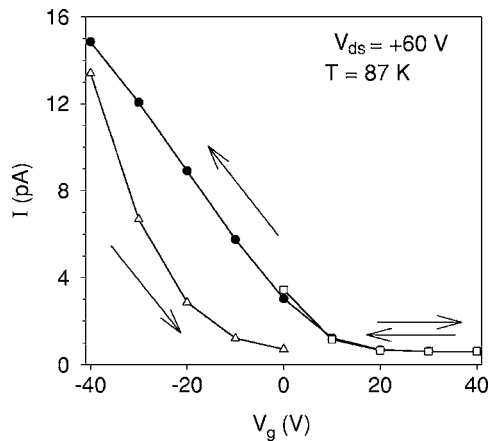
FIG. 3. Dark current, I, at 87 K as a function of applied gate voltage with $V_{ds}=+60$ V. V_g is swept from 0 V to +40 V (open squares), from +40 V to −40 V (filled circles), and finally from −40 V to 0 V (open triangles). The solid lines are guides to the eye.

+60 V than on the way down from +60 V to −60 V. Thus, the current apparently decays with time at these low temperatures; data points are taken every 10 s, giving a time scale to the hysteresis. For the I-V curves in the main part of Fig. 2 the data shown are for the voltage sweep from 0 V to +60 V and the sweep from 0 V to −60 V in order to display the current before it decays.

Figure 3 shows the dark current as a function of V_g, with $V_{ds}=+60$ V. Consistent with the data in Fig. 2, the current is largest at negative V_g and suppressed at positive V_g. The current is roughly linear with V_g when it is varied from 0 V to −40 V, but is smaller in magnitude on the way back from −40 V to 0 V.

Figure 4 shows the I-V curves for the dark current before (top panels) and after (lower panels) chemical treatment with butylamine at 295 K [Fig. 4(a)] and at 87 K [Fig. 4(b)]. In all four plots of Fig. 4 V_{ds} is swept from 0 V to +100 V (open squares), +100 V to −100 V (open circles), and finally from −100 V back to 0 V (open triangles). Note the different scales in the two panels of Fig. 4(a): The dark current at 295 K is approximately three orders of magnitude higher after treatment with butylamine. By contrast, at 87 K [Fig. 4(b)], the dark current decreases rather than increases with butylamine treatment. Whereas the current is hysteretic and measurable only for positive V_g at 87 K, it shows little hysteresis and is nearly symmetric with V_{ds} at 295 K.

Differential conductance measurements at room temperature as a function of gate voltage are displayed in Fig. 5 for a sample treated with butylamine. To measure the differential conductance we apply a small ac voltage of $2V_{rms}$ at 13 Hz in series with a dc voltage of $|V_{ds}|=110$ V across the electrodes (the electrodes are spaced by 2 μm for the data in Fig. 5). The gate voltage is stepped in increments of 5 V. To minimize the hysteresis, we apply V_g for 5 s and return V_g to 0 for 5 s for each data point. This effectively is a measurement of how the slope of the I-V_{ds} curve at $|V_{ds}|=110$ V varies with gate voltage. For both positive and negative V_{ds} the differential conductance increases with increasing negative V_g and decreases with positive V_g.

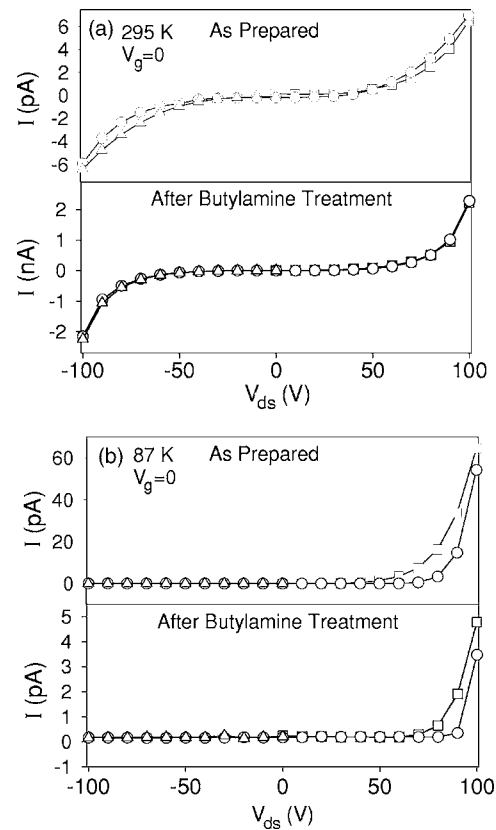The temperature, T, dependence of the dark current at $V_{ds}=−90, −80, −70, −60, −50,$ and −40 V for a butylamine

FIG. 4. Dark current, I, before (top panels) and after (bottom panels) treatment with butylamine at (a) 295 K and (b) 87 K with $V_g=0$. V_{ds} is swept from 0 V to +100 V (open squares), from +100 V to −100 V (open circles), and finally from −100 V to 0 V (open triangles). Solid lines serve as guides to the eye. Note that the current at 295 K increases by almost 1000 times after treatment.

treated sample is plotted in Fig. 6. The dark current is linear with inverse temperature when plotted on a semilogarithmic graph, indicating Arrhenius behavior. Solid lines are fits to the Arrhenius equation at each voltage. The current noise of our electrometer is ∼0.01 pA, indicating that except at the most negative voltages, there is no evidence for anything other than a simply activated current. From the fits the activation energy at each voltage is determined, and the activation energy is plotted versus electric field in the inset of Fig. 6 and fit to a straight line. The y intercept of the line gives the zero-field activation energy for the dark current and is found to be 0.38±0.02 eV. From the slope of the line the distance traveled during the rate-limiting step in the activated process can be calculated

$$\Delta E = el\varepsilon, \qquad (1)$$

where ΔE is the activation energy, e is the charge of the electron, l is distance, and ε is electric field. From the fit of the inset of Fig. 6 we find $l=2.2\pm0.2$ nm. We note that before butylamine treatment, the conductance is too small to measure the T dependence.

Figure 7 demonstrates that both the room temperature dark current, I, and the low temperature photocurrent, ΔI, depend only on electric field, and not independently on the
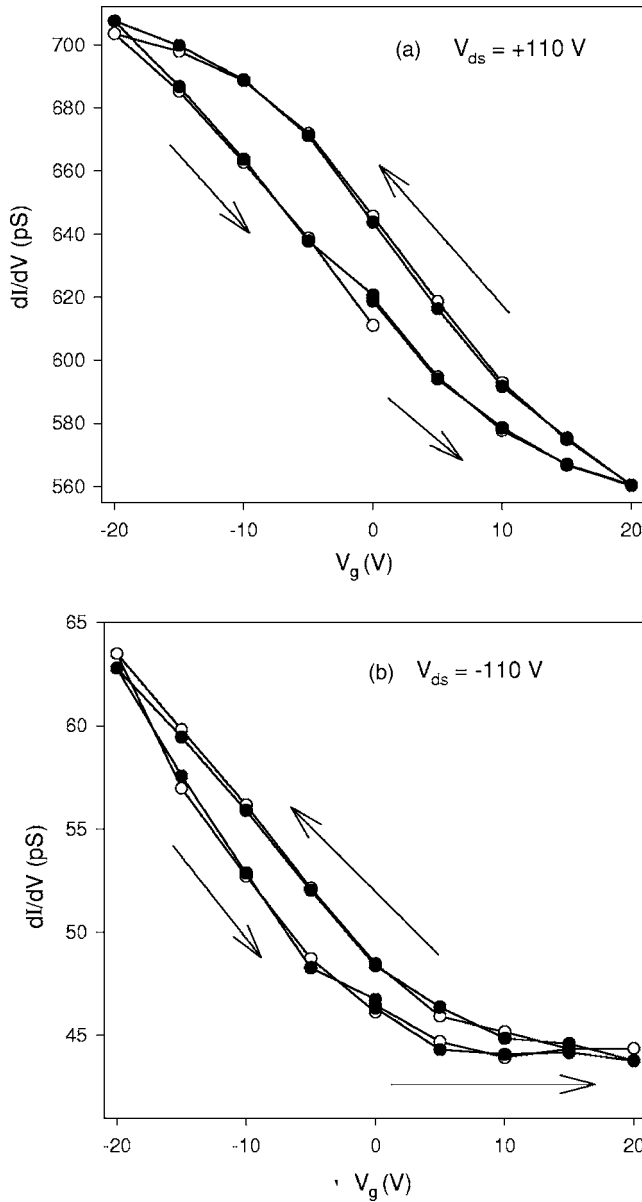
FIG. 5. (a) Differential conductance, dI/dV, as a function of V_g with (a) $V_{ds}=+110$ V and (b) $V_{ds}=-110$ V. V_g is applied for 5 s followed by a recovery period of 5 s at each value of V_g. V_g is varied from 0 V to +20 V, from +20 V to −20 V, and finally from −20 V to 0 V. V_{ac} is 2 V_{rms} at a frequency of 13 Hz. In (a) and (b) the open circles are the first V_g cycle and the closed circles are the second cycle.

separation of the electrodes. We define ΔI as the difference between the dark and photocurrents, since the dark current is in general 2–3 orders of magnitude less than the photocurrent, ΔI and the absolute photocurrent are essentially identical. The current is measured across electrodes with gaps of 1 μm and 2 μm and is found to be the same magnitude for a given field. The sample used for Fig. 7 was deposited onto gold electrodes patterned on a quartz substrate and has no back gate. This was done in order to minimize field drop to the gate and better observe the field scaling effect.

The photocurrent, ΔI vs V_{ds} at 87 K and 295 K are given in Fig. 8 for both untreated (a) and butylamine-treated (b)
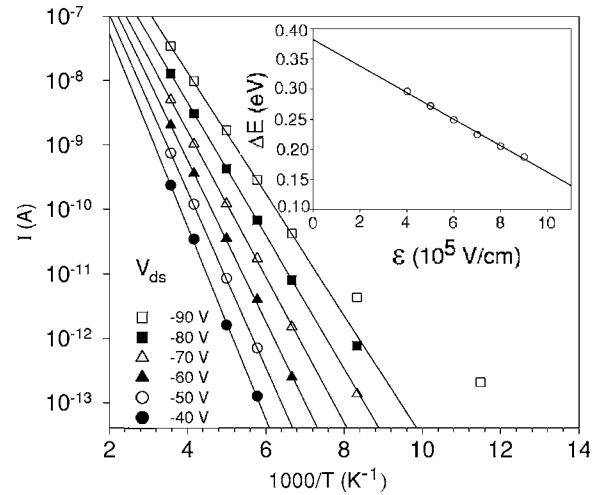

FIG. 6. Temperature dependence of the dark current, I, (butylamine treated) at various values of V_{ds} with $V_g=0$. The solid lines are Arrhenius fits to the data at each voltage. The inset is a plot of the activation energy, ΔE, as a function of field, $\varepsilon = V_{ds}/L$, where L is the electrode separation. The solid line in the inset is linear fit to the activation energy versus field data.

films. The axis for the photocurrent at each temperature is scaled to show that the shape of the two I-V curves is the same. The intensity of the excitation light is 30 mW/cm^2. The insets are included to emphasize how the magnitude of the photocurrent varies with T. The magnitude of the photocurrent increases with treatment at both temperatures. However, as seen in the insets, the temperature dependence after treatment is opposite to that before treatment; the magnitude of the photocurrent before treatment increases as T decreases, whereas after treatment it decreases with T. For all
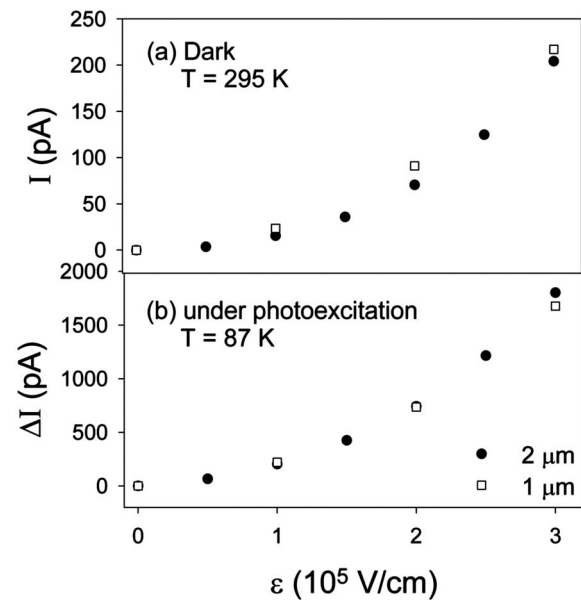

FIG. 7. (a) Dark current, I, at 295 K (b) and photocurrent, ΔI, at 87 K and $V_g=0$ measured on a 1 μm gap (open squares) and on a 2 μm gap (closed circles) and plotted versus electric field, $\varepsilon = V_{ds}/L$, where L is the gap between the electrodes.
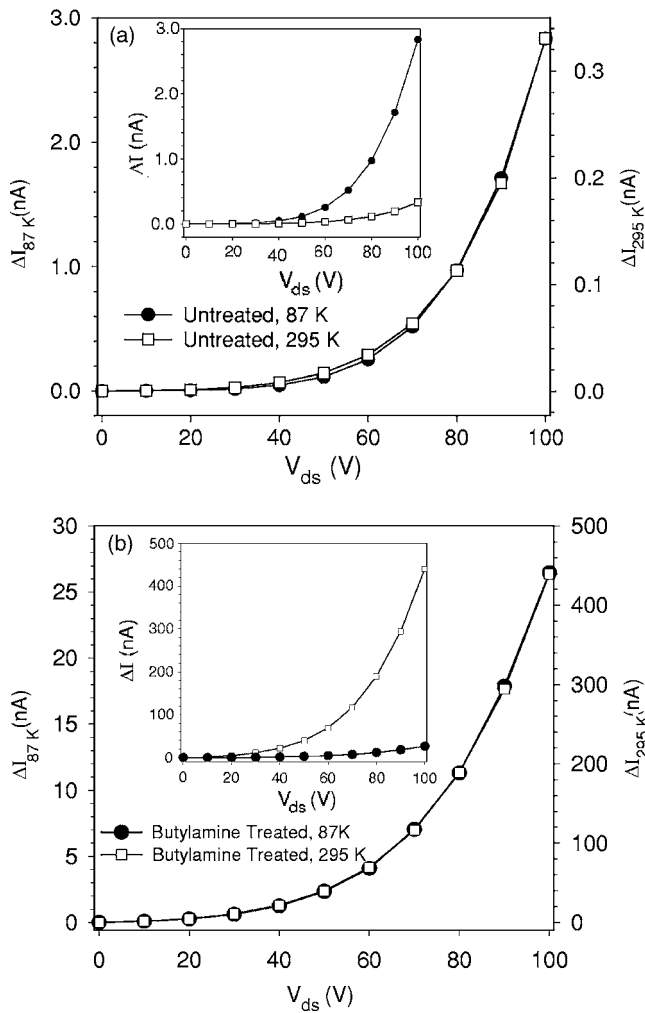
FIG. 8. (a) Photocurrent, ΔI, at 87 K (filled circles and left axis) and at 295 K (open squares and right axis) before treatment with butylamine ($V_g=0$). Each axis is scaled to illustrate the similar shape of the ΔI-V curves at the two temperatures. The inset in (a) is the data plotted with a shared y axis to illustrate the difference in the magnitude of the current at the two temperatures. (b) Photocurrent at 87 K (filled circles and left axis) and at 295 K (open squares and right axis) after treatment with butylamine ($V_g=0$). The inset in (b) is the data plotted with a shared y axis. Solid lines are guides to the eye. The photoexcitation intensity is 30 mW/cm^2.

data in Fig. 8 V_{ds} is swept from 0 V to +100 V. Though not shown, ΔI in all plots is symmetric in V_{ds} and displays little hysteresis.

Figure 9 shows the dependence of ΔI on photoexcitation intensity. $V_{ds}=+100$ V is applied to the sample while the photoexcitation intensity is stepped. Measurements are performed on the CdTe NC film after butylamine treatment at 87 K (closed circles) and room temperature (open circles). The photoexcitation intensity dependence of the current is closer to linear at 87 K than at room temperature.

Figure 10 shows the decay of ΔI after the excitation light is turned off at room temperature and 87 K. V_{ds} is held at -90 V and the photoexcitation intensity of the light is 30 mW/cm^2. The photocurrent decay is faster at room temperature than at 87 K.
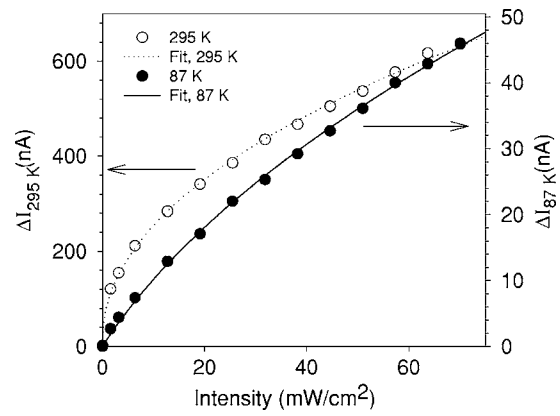

FIG. 9. The photoexcitation intensity dependence of ΔI. Data at 87 K and 295 K are represented by filled circles and open circles, respectively. The solid line is a fit to the 87 K data, and the dotted line is a fit to the 295 K data, as discussed in the text. The sample has been treated with butylamine; $V_{ds}=+100$ V and $V_g=0$.

The results presented in Figs. 2–10 depict trends which have been observed on all CdTe NC film samples measured to date. The magnitude of the current varies slightly from sample to sample due to differences in sample thickness but the I vs V_{ds} curves all display the same response to temperature, butylamine treatment, photoexcitation, and gate voltage. Three batches of CdTe NC's were synthesized and 2–3
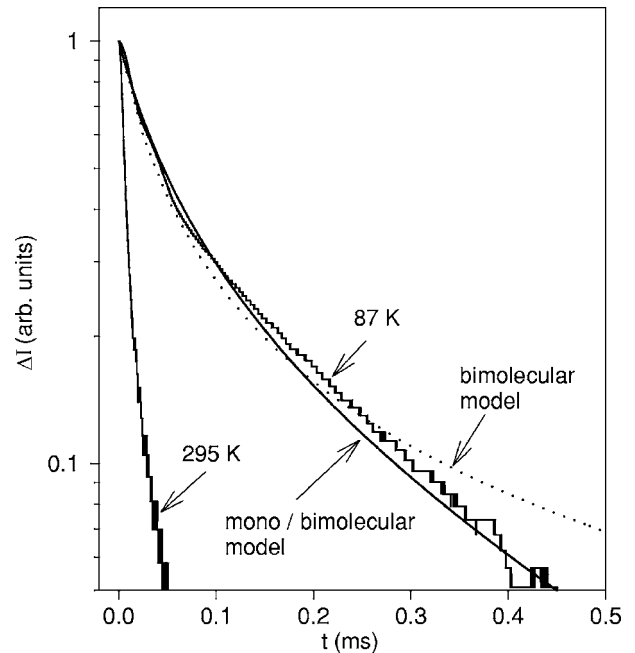

FIG. 10. The photocurrent, ΔI, decay at 295 K and 87 K for a sample treated with butylamine. $V_{ds}=-90$ V, $V_g=0$, and the excitation intensity is 30 mW/cm^2 before the photoexcitation is removed. The curve furthest to the right is the photocurrent decay at 87 K while the curve to the left is the photocurrent decay at 295 K. The decay at 87 K is fit with a model for bimolecular recombination (dotted line) and a model for a combination of bimolecular and monomolecular recombination (solid line) as described in the text. The decay at 295 K is, for the most part, faster than the resolution of the current amplifier used for the measurement.

samples prepared from each batch. Eight samples were measured in total. On each sample 3 separate 1 or 2 μm gaps were tested. In this paper, Figs. 2 and 3 (which demonstrate the gate dependence of the CdTe NC film) are from the same sample. Figs. 4 and 8–10 show the behavior of the dark and photocurrent after chemical treatment and are from the same sample. Figs. 5–7 were measured at a later time and each show data taken from separate samples.

IV. DISCUSSION

Previous studies of charge transport in close-packed CdSe NC films, performed on inverted FET structures, found that current resulting from the injection of electrons was on the order of picoamps at $V_{ds} \sim 100$ V and decayed with time after application of the voltage. The number of electrons injected was affected by the gate but this current also decayed over time.[21,28] Even after treatment with basic molecules, which were shown to decrease the inderdot spacing, no steady-state dark current was observed in the CdSe NC films.[22] In the present work we find that at low temperature CdTe NC films, like CdSe NC films, display transient dark current on the order of picoamps. However, unlike CdSe NC films the room temperature dark current in CdTe NC films is steady state.

Charge transport in close-packed NC films is expected to be limited by tunneling between dots and to therefore have a strong dependence on the interdot spacing.[18,19,22] Treatment with butylamine has been shown to enhance photoconductivity in CdSe NC films by decreasing interparticle spacing from ~ 1.1 nm before treatment to ~ 0.2 nm after treatment.[22] Similarly, we find that treatment with butylamine increases the room temperature dark conductance in CdTe NC films by more than three orders of magnitude (Fig. 4). The dark current after treatment with butylamine treatment is large enough for us to measure the differential conductance as a function of gate voltage. Figure 5 shows that the differential conductance at both positive and negative V_{ds} increases with increasing negative V_g and decreases with positive V_g. That we see no increase in differential conductance even at quite large positive V_g suggests that the electrons' contribution to the current is small. This indicates that holes are the majority carriers.

The low temperature dark current is also most likely carried by holes. Dark current is only present at positive drain bias and increases with the application of a negative gate bias (Figs. 2 and 3), consistent with hole conduction in a FET. The observed hysteresis could be a result of charge build up at the injecting contact[28] or of the opening and closing of conducting channels between the electrodes.[29]

The temperature dependence of the dark current, after treatment with butylamine, suggests that the hole density is thermally activated (Fig. 6). The zero-field activation energy (from the inset of Fig. 6) is 0.38 ± 0.02 eV. This is smaller than half of the estimated band edge energy of 1.8 eV needed to create an electron-hole pair thermally. We infer that the current is limited by the release of holes from traps. The room temperature dark current I-V curve is nearly symmetric and displays little hysteresis at room temperature [Fig. 4(a)].

Since we have demonstrated that holes are the dominant carrier, we ascribe the symmetric V_{ds} dependence to the field dependence of the mobility of the holes, as well as that of their activation energy, as discussed in detail after we discuss the photoconductance.

As reported previously by Jarosz *et al.*,[22] the photocurrent in CdSe NC films after chemical treatment displays saturation with applied field when every photogenerated carrier reaches an electrode before recombining. The photoconductive gain is found to be equal to unity for this system, and this indicates that the gold electrodes form blocking contact with the CdSe NC film. The current for these films is found to saturate at lower applied voltages at 87 K than at room temperature because the exciton lives longer at lower T and the probability of ionization at a given field is therefore larger. This higher ionization probability also explains why the photocurrent in CdSe NC films is larger at low T than high T.

Before treatment with butylamine, the photocurrent in CdTe NC films [Fig. 8(a)] increases with decreasing T, as well. However, after treatment the photocurrent at 295 K is *higher* than the photocurrent at 87 K [Fig. 8(b)]. Furthermore, saturation is not observed at either temperature. At the fields used it is unlikely that the current is limited by field ionization of the exciton. In addition, the magnitude of the current is higher than expected for a photoconductive gain of unity. We infer that the photocurrent in CdTe NC films is a secondary photocurrent rather than a primary photocurrent as observed in CdSe NC films.

Secondary photocurrents occur when the contacts can inject electrons, holes, or both.[23] The dark current in CdTe NC films is carried by holes, as discussed above, and these holes must be replenished from the gold electrodes to maintain a steady-state current. Assuming that both carriers are mobile but that only the hole is replenished at the electrodes, the gain does not saturate at unity. Holes contribute to the current until the electron reaches the electrode or recombines with a hole. The lifetime of the hole is thus equal to the lifetime of the electron. At high fields the electron reaches the electrode and the lifetimes of both the electron and the hole equal the transit time of the electron,

$$\tau_p = \tau_n = T_n = \frac{L^2}{\mu_n V}, \qquad (2)$$

where τ_p is the hole lifetime, τ_n is the electron lifetime, T_n is the transit time of the electrons, L is the width of the gap, μ_n is the electron mobility, and V is the applied voltage. The photoconductive gain, G, becomes a function of the mobility of the two carriers.[23]

$$G \approx \frac{\mu_p}{\mu_n}. \qquad (3)$$

Therefore the gain is expected to be greater than unity if the mobility of the hole is greater than that of the electron.

Given the excitation intensity, sample area, optical absorption of the film, exciton separation efficiency (assumed to be 1) and a gain of unity, we estimate the maximum primary photocurrent expected in the CdTe NC film to be ap-

proximately 40 nA. The current at 100 V and room temperature is 440 nA, resulting in a photoconductive gain of about 10. Were the electron more mobile than the hole, as it is in bulk CdTe,[30] the gain would be less than unity. Thus the hole has a higher mobility than the electron in the CdTe NC film and holes effectively cycle through the circuit for a time equal to the recombination time. The concept of a hole is particular to a semiconductor and they do not actually travel in the external measurement circuit. However, the motion of holes in the film of CdTe NCs influences the flow of electrons in the external circuit. A hole leaving the NC film corresponds to an electron entering the film and vice versa. At 100 V, 10 holes enter and exit the film before recombining with the photogenerated electron and thus travel an effective distance of $\sim 10^{-3}$ cm. The recombination lifetime is faster than the resolution of our current amplifier at room temperature, giving an upper bound on the lifetime of 10 μs. From this information, we find a lower limit on the hole mobility of $\sim 10^{-4}$ cm^2/V s at 100 V.

The photoexcitation intensity dependence of the photocurrent (Fig. 9), fit using the procedure outlined by Jarosz *et al.*, provides information about the recombination mechanism.[20,23] Photogenerated holes, of density n, can either recombine with the equal density of photogenerated electrons or with the pre-existing trapped electrons, of density N_t,

$$F = (N_t + n)nb, \qquad (4)$$

where F is the carrier photogeneration rate, proportional to photoexcitation intensity, and b is the bimolecular recombination coefficient. In CdSe NC films it has been suggested that holes are trapped in surface states such as unpassivated selenium and electrons (the counter charge) are deeply trapped on SeO$_2$.[20] By analogy we speculate that CdTe NC films most likely contain holes trapped in unpassivated Te sites and trapped electrons in TeO$_2$. If N_t is much larger than n the current, proportional to the hole concentration, is linear in photoexcitation intensity, while if n is larger than N_t the current is proportional to the square root of the photoexcitation intensity. Fitting Eq. (4) to the data at low temperature in Fig. 9 we find $\frac{n}{N_t}=1.34$, indicating that holes recombine with both free and trapped electrons, approximately equally. At 295 K the fit is poor because $\frac{n}{N_t}$ is so large. When the data is instead fit to a power law, as designated by the dotted line in Fig. 9, the exponent is 0.5, as expected for bimolecular recombination.

When recombination involves both photogenerated and trapped carriers, the current decay from steady state, after light excitation is removed, is predicted to follow

$$\frac{n}{n_o} = \frac{\exp(-N_t bt)}{1 + \frac{n_o b}{N_t b}(1-\exp(-N_t bt))}, \qquad (5)$$

where n_o is initial carrier density, and t is the time after removal of photoexcitation.[23] We fit the low temperature data in Fig. 10 with Eq. (5), as well as the bimolecular form, obtained by taking the limit of $N_t b \rightarrow 0$. Equation (5) is a better fit, confirming that recombination of holes with
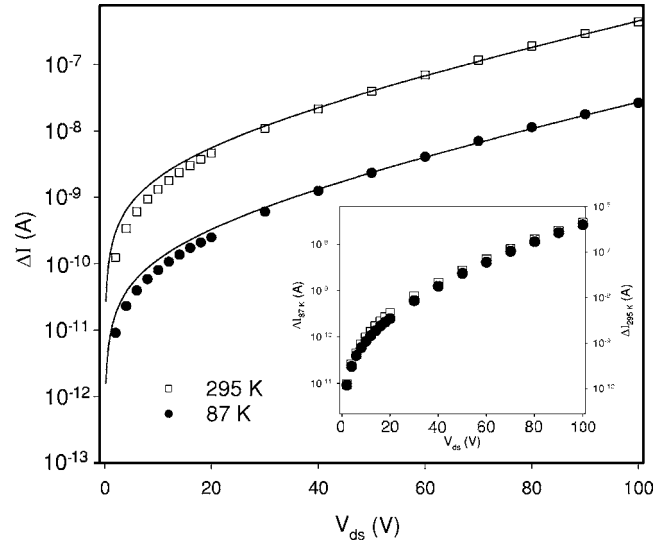

FIG. 11. A semilogarithmic plot of the photocurrent, ΔI versus V_{ds} with $V_g=0$ at 295 K (open circles) and 87 K (closed circles). The solid lines are fits to Eq. (6). The data are scaled in the inset to show that the field dependence is independent of temperature.

trapped electrons is significant at low temperatures. From the fit $\tau=(N_t b)^{-1}=340$ μs and $(n_o b)^{-1}=55$ μs. Most of the room temperature photocurrent decay is faster than the 10 μs rise-time of the current amplifier. Though the decay could not be fit with the bimolecular form of Eq. (5), an increase in the decay rate supports the concept that trapping plays a smaller role as the temperature increases.

The transient dark current in films of annealed CdSe has a voltage dependence at fixed time that is well described by the following phenomenological expression[21]

$$\Delta I \approx \frac{V_{ds}}{R_o} \exp\left(\frac{|V_{ds}|}{V_o} \right). \qquad (6)$$

Here R_o is a characteristic resistance and V_o is a characteristic voltage. We fit (Fig. 11) the photocurrent data to Eq. (6) and find good agreement with $V_o=29$ V for both 87 K and 295 K. This corresponds to an energy difference from one NC to its neighbor of ~ 175 meV (determined by dividing V_o by the number of NCs which fit across 1 μm), similar to the value found in annealed CdSe NC films.[21] R_o at 87 K is 1.2×10^{11} Ω and R_o at 295 K is 7.2×10^9 Ω. The temperature dependence of R_o is consistent with the increased importance of monomolecular recombination at low T. The observation that this simple phenomenological model describes the voltage dependence of the photocurrent so well, with the same value of V_o at low and high T is very important. As discussed above, the fields are high enough that all excitons are ionized. Therefore, the voltage dependence of Eq. (6) comes from that of the mobility, and the field dependence of the mobility of the holes is well described by

$$\mu \propto \exp\left(\frac{|\varepsilon|}{\varepsilon_o} \right), \qquad (7)$$

where ε_0 is a characteristic electric field. However, as in the case of CdSe NC films, the field scale ε_0 is too small to be explained by a simple tunneling model.[21]
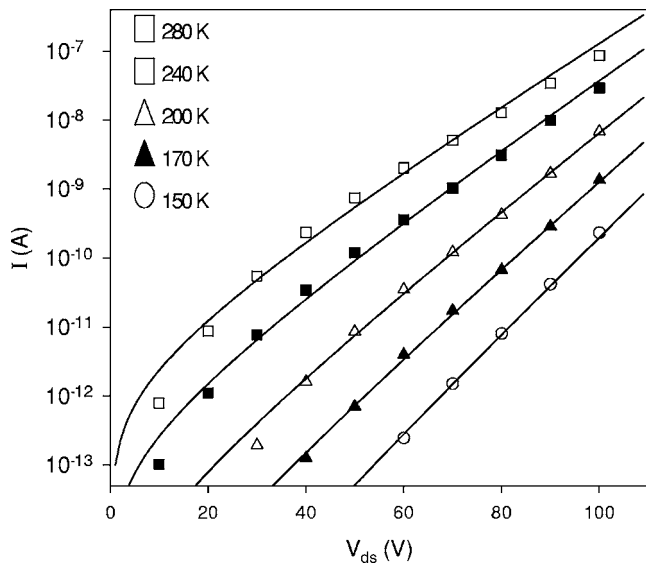
FIG. 12. Dark current, I versus V_{ds} at various temperatures with $V_g = 0$. The solid lines are fits as described in the text.

This inspires us to describe the steady-state dark current in the same way: As discussed above, the holes are thermally released from traps with an activation energy that decreases linearly with voltage (see Fig. 6). Assuming that the holes, once released from traps have the field-dependent mobility described by Eq. (7) we predict that the dark current will be

$$I = \frac{V_{ds}}{R_o} \exp\left(\frac{V_{ds}}{V_o} + \frac{aV_{ds} - \Delta E_0}{kT} \right), \qquad (8)$$

where ΔE_0 is the zero-field activation energy, k is Boltzmann's constant, and $a = l/L$ [see Eq (1)]. In Fig. 12 we use this form to fit the I-V_{ds} curves at each temperature. We set $V_o = 29$ eV from the photocurrent data and then fit the data at 150 K and 280 K to Eq. (8) by adjusting R_o and ΔE_0,

until both data sets are fit by varying only the temperature. For the best fit $R_o = 5 \times 10^6$ Ω, $a = 1.5 \times 10^{-3}$, and $\Delta E_0 = 0.34 \pm 0.02$ eV. ΔE_0 is close to the value 0.38 ± 0.02 eVvalue determined from the inset of Fig. 5. R_o, a, ΔE_0, and V_o are all held constant in the fits at 240, 200, and 170 K. The agreement of this phenomenological expression with the data is remarkable.

V. CONCLUSIONS

Our studies of the transport properties of CdTe NC films in FET structures lead to the following conclusions which are generally true for CdTe NC films contacting gold electrodes:

(1) The current is carried by holes, both in the dark and under photoexcitation.

(2) The secondary photocurrent measured in the CdTe NC films, made possible by the nonblocking gold electrodes, gives a gain greater than unity, showing that holes have a higher mobility than electrons.

(3) The voltage dependence of the photocurrent is temperature independent and leads to a simple phenomenological description of the voltage dependence of the hole mobility.

(4) The dark current is thermally activated with an energy that decreases linearly with voltage. The voltage dependence of the mobility, extracted from the photocurrent, is the same as that of the dark current.

[1] E. G. Soltesz, S. Kim, R. G. Laurence, A. M. DeGrand, C. P. Parungo, D. M. Dor, L. H. Cohn, M. G. Bawendi, J. V. Frangioni, and T. Mihaljevic, Ann. Thorac. Surg. **79**, 269 (2005).

[2] C. P. Parungo, S. Ohnishi, S.-W. Kim, S. Kim, R. G. Laurence, E. G. Soltesz, F. Y. Chen, Y. L. Colson, L. H. Cohn, M. G. Bawendi, and J. V. Frangioni, J. Thorac. Cardiovasc. Surg. **129**, 844 (2005).

[3] C. P. Parungo, Y. L. Colson, S.-W. Kim, S. Kim, L. H. Cohn, M. G. Bawendi, and J. V. Frangioni, Chest **127**, 1799 (2005).

[4] M. Dahan, S. Levi, C. Luccardini, P. Rostaing, B. Riveau, and A. Triller, Science **302**, 442 (2003).

[5] D. R. Larson, W. R. Zipfel, R. M. Williams, S. W. Clark, M. P. Bruchez, F. W. Wise, and W. W. Webb, Science **300**, 1434 (2003).

[6] J. K. Jaiswal, H. Mattoussi, J. M. Mauro, and S. M. Simon, Nat. Biotechnol. **21**, 47 (2003).

[7] B. Dubertret, P. Skourides, D. J. Norris, V. Noireaux, A. H. Brivanlou, and A. Libchaber, Science **298**, 1759 (2002).

[8] S. Kim, Y. T. Lim, E. G. Soltesz, A. M. De Grand, J. Lee, A. Nakayama, J. A. Parker, T. Mihaljevic, R. G. Laurence, D. M. Dor, L. H. Cohn, M. G. Bawendi, and J. V. Frangioni, Nat. Biotechnol. **22**, 93 (2004).

[9] H.-J. Eisler, V. C. Sundar, M. G. Bawendi, M. Walsh, H. I. Smith, and V. Klimov, Appl. Phys. Lett. **80**, 4614 (2002).

[10] V. C. Sundar, H.-J. Eisler, and M. G. Bawendi, Adv. Mater. (Weinheim, Ger.) **14**, 739 (2002).

[11] V. C. Sundar, H. J. Eisler, T. Deng, Y. Chan, E. L. Thomas, and M. G. Bawendi, Adv. Mater. (Weinheim, Ger.) **16**, 2137 (2004).

[12] P. T. Snee, Y. Chan, D. G. Nocera, and M. G. Bawendi, Adv. Mater. (Weinheim, Ger.) **17**, 1131 (2005).

[13] Y. Chan, J. S. Steckel, P. T. Snee, J. M. Caruge, J. M. Hodgkiss, D. G. Nocera, and M. G. Bawendi, Appl. Phys. Lett. **86**, 073102 (2005).

[14] Y. Chan, J. M. Caruge, P. T. Snee, and M. G. Bawendi, Appl. Phys. Lett. **85**, 2451 (2004).

[15] P. Guyot-Sionnest and C. Wang, J. Phys. Chem. B **107**, 7355

(2003).

[16] D. Yu, C. J. Wang, and P. Guyot-Sionnest, Science **300**, 1277 (2003).

[17] B. L. Wehrenberg and P. Guyot-Sionnest, J. Am. Chem. Soc. **125**, 7806 (2003).

[18] C. Kagan, Ph.D. thesis, Massachusetts Institute of Technology, Cambridge, 1996.

[19] C. A. Leatherdale, C. R. Kagan, N. Y. Morgan, S. A. Empedocles, M. A. Kastner, and M. G. Bawendi, Phys. Rev. B **62**, 2669 (2000).

[20] M. V. Jarosz, N. E. Stott, M. Drndic, N. Y. Morgan, M. A. Kastner, and M. G. Bawendi, J. Phys. Chem. B **107**, 12585 (2003).

[21] M. Drndic, M. V. Jarosz, N. Y. Morgan, M. A. Kastner, and M. G. Bawendi, J. Appl. Phys. **92**, 7498 (2002).

[22] M. V. Jarosz, V. J. Porter, B. R. Fisher, M. A. Kastner, and M. G. Bawendi, Phys. Rev. B **70**, 195327 (2004).

[23] R. H. Bube, *Photoconductivity of Solids* (Wiley, New York, 1960).

[24] C. B. Murray, D. J. Norris, and M. G. Bawendi, J. Am. Chem. Soc. **115**, 8706 (1993).

[25] C. B. Murray, C. R. Kagan, and M. G. Bawendi, Science **270**, 1335 (1995).

[26] C. B. Murray, C. R. Kagan, and M. G. Bawendi, Annu. Rev. Mater. Sci. **30**, 545 (2000).

[27] C. R. Kagan, C. B. Murray, M. Nirmal, and M. G. Bawendi, Phys. Rev. Lett. **76**, 1517 (1996).

[28] N. Y. Morgan, C. A. Leatherdale, M. Drndic, M. V. Jarosz, M. A. Kastner, and M. Bawendi, Phys. Rev. B **66**, 075339 (2002).

[29] D. S. Novikov, M. Drndic, L. S. Levitov, M. A. Kastner, M. V. Jarosz, and M. G. Bawendi, Phys. Rev. B **72**, 075309 (2005).

[30] H. Landolt and R. Bornestein, *Numerical Data and Functional Relationships in Science and Technology* (Springer-Verlag, Berlin, 1961).